Spherically Smooth Cathode Particles by Mechanofusion Processing

View the article online for updates and enhancements.

Spherically Smooth Cathode Particles by Mechanofusion Processing

Lituo Zheng,[1,*] Congxiao Wei,[1,*] M. D. L. Garayt,[1] Judy MacInnis,[2] and M. N. Obrovac ●[1,3,**,z]

[1]*Department of Chemistry, Dalhousie University, Halifax NS B3H 4R2, Canada*
[2]*Department of Chemistry, Cape Breton University, Sydney NS B1P 6L2, Canada*
[3]*Department of Physics and Atmospheric Science, Dalhousie University, Halifax NS B3H 4R2, Canada*

Surface modification has been shown to be useful for improving the cycling performance of cathode materials. Typically hetero-compositional coatings are applied on cathode particle surfaces using methods, such as aqueous deposition and atomic layer deposition (ALD), that can be expensive and inefficient. In this report, a dry mechanofusion method was used to treat cathode particles with no auxiliary coating applied. This resulted in a drastic reduction in surface area and the elimination of surface features on the particles. Furthermore, the processing results in an iso-compositional amorphous shell on the surface of each particle. The resulting particles have improved cycling. We believe the mechanofusion process is an important step toward the goal of improving the cycling performance of cathode materials.

Commercial rechargeable lithium-ion (Li-ion) batteries typically use a lithium transition metal oxide cathode and a graphite anode.[1] For the past few decades, most advances in energy density have been results of engineering and cell design. However, conventional Li-ion batteries are approaching their theoretical energy density limit.[2] New materials solutions are now needed to further increase energy density and cycle life.[3]

Surface chemistry plays an important role in cycling performance.[4] The deterioration of electrolyte on active material surfaces is one of the key issues that lead to cell fade.[5] The use of electrolyte additives and advanced salts can greatly reduce the electrolyte decomposition and lead to better cycle life.[6] Cycle life can also be improved significantly by modifying the interface between active material and the electrolyte. For example, a core-shell cathode material that contains a nickel-rich core and manganese-rich shell can offer better cyclability than tranditional nickel-rich materials, due to the more stable manganese-rich surface.[7] It can also be advantageous to apply an inactive coating layer, such as Al_2O_3, to cathode particles to create a more stable interface with battery electrolytes and to improve cycling performance.[8] Such surface coatings can also improve cathode performance at higher operating potentials, thereby increasing cell energy density. Methods, such as atomic layer deposition (ALD) and wet chemistry may be used to uniformly coat cathode particles.[9,10] However, wet methods produce waste liquid and require filtering and additional drying/heating steps, while ALD is expensive and difficult to scale up.

Physical methods that employ dry processing are environmentally friendly and advantageous for industrial use because of the elimination of the use of solvents. The mechanofusion (MF) method uses a high shear field to spheronize or surface-coat powders without using any liquids. Figure 1 shows a schematic diagram of a working MF machine. The machine consists of a chamber where powder samples are placed, a rounded press head with a constant gap between the press head and the chamber, and a scraper with a smaller gap between the chamber. During operation, the sample chamber rotates while the other parts are immobilized. As the chamber rotates at high speed, powder samples are pressed against the chamber wall by centrifugal force and forced through the narrow gap between press head and chamber. This results in high compression and shear forces applied to the powder samples. The MF process is typically used for the spheronization of irregularly shaped particles or for coating small particles onto larger particles.[11]

Several publications describe particles that have been spheronized or coated with another phase by the MF method.[12–15] We have used the MF process previously to apply Al_2O_3 surface coatings to cathode particles.[16]

Transition metal oxide cathode materials are often synthesized from co-precipitated precursors.[17,18] Co-precipitation results in spherical hydroxide precursors with transition metals homogeneously mixed at an atomic level. The resulting synthesized cathode materials are typically in the form of polycrystalline powders or particulate spheres that are about $5-30\,\mu m$ in size in which each powder particle consists of an aggregate of crystallites with grain sizes in the range of $0.2-1\,\mu m$.[19] Such polycrystalline cathode particles contain surface features in the form of pits and valleys whose depth is on the order of the same size as their crystallite size. As a consequence, the particles have a relatively high surface area, which in turn increases reactivity with electrolytes in battery applications, leading to capacity loss. Therefore, surface area reduction is another approach that could reduce surface reactions and improve cycle life.[20] To our knowledge, post-processing of polycrystalline cathode particles to reduce their surface area has not been explored as a method to increase cycle life.

Here, we present a study showing that MF processing can reduce the surface area and improve the cycling performance of commercial polycrystalline $LiNi_{0.6}Mn_{0.2}Co_{0.2}O_2$ (NMC622). This cathode material was MF processed neat, without the use of additives. The resulting materials have a smoothed surface and an amorphous thin coating layer
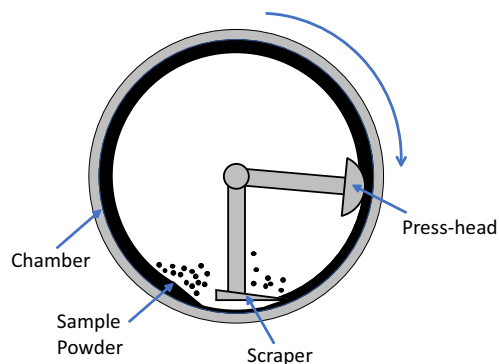

Figure 1. A schematic diagram of a working mechanofusion machine.

*Electrochemical Society Student Member.
**Electrochemical Society Member.
zE-mail: mark.obrovac@dal.ca

with the same composition as the bulk material. These materials were found to have significantly improved cycling retention in lithium cells.

Experimental

Commercial NMC622 powders (obtained from a reputable manufacturer) were used directly without further treatment in this study. MF was conducted using a Hosokawa AM-15F mechanofusion system. NMC622 with a total tapped powder volume of ~50 mL was added to the processing vessel. MF was conducted with a press-head gap of 1 mm, a scraper gap of ~0.4 mm, and a rotation speed of ~1800 rpm. Samples were collected from the vessel after MF processing for different time periods. The morphology and elemental distribution of samples were measured using a field emission scanning electron microscope (FESEM, TESCAN MIRA 3). Cross-sections of samples were prepared using a cross-section polisher (JEOL, IB-19530CP). X-ray diffraction (XRD) patterns were recorded with a Rigaku Ultima IV X-ray diffractometer equipped with a Cu anode X-ray tube, a scintillation detector, and a diffracted beam monochromator. Transmission electron microscopy (TEM) was conducted using a Hitachi 7700 with Exalens. To prepare TEM samples, a small amount of cathode powder was added to ethanol and the dispersion was sonicated for 15 min to separate the particles. A drop of the stable solution was added to the formvar/carbon TEM grid and allowed to air dry. The measurements were conducted in high contrast mode using an accelerating voltage of 80.0 kV and a LaB_6 emission current of 8.0 μA.

Electrodes were made from slurries containing active materials, PVDF binder (polyvinylidene fluoride, Kynar HSV 900), carbon black (Super C65, Imerys Graphite and Carbon) in a 96:2:2 weight ratio, and an appropriate amount of N-methyl 2-pyrrolidone (Sigma Aldrich, anhydrous 99.5%). Slurries were mixed using a Mazerustar planetary mixer. The mixed slurries were coated onto aluminum foil using a coating bar with a 0.015 cm gap and dried at 120°C in air. The coating was calendered and circular electrode disks were punched from the coating and dried under vacuum at 120°C overnight before cell

assembly. Coin cells (2325-size) were assembled with two Celgard 2300 and one polypropylene blown microfiber separator (3M Company) as separators, and lithium foil as the counter/reference electrode. The diameter of the working electrode, separator and lithium foil were 13 mm, 23 mm, and 18 mm, respectively. The typical loading of active material was ~10 mg/cm^2 and the electrode coating thickness was ~50 μm. 1 M $LiPF_6$ in a solution of ethylene carbonate and diethyl carbonate (volume ratio 1:2, from BASF) was used as electrolyte for collecting the voltage curve, and 1 M $LiPF_6$ in a solution of fluoroethylene carbonate and dimethyl carbonate (volume ratio 1:4, from BASF) was used as electrolyte for the cell cycling tests. Cells were cycled at 30.0 ± 0.1°C with a Maccor Series 4000 Automated Test System. Cells were cycled between 3.0 V and 4.4 V. A current rate of C/20 was used for the first cycle, and for subsequent cycles, a C/2 rate was used with a 5 hour hold at the top of charge. Two cells were made for each material and all duplicate cells were found to be in good agreement.

Results and Discussion

Figure 2a shows an SEM image of a pristine NMC622 particle prior to MF processing. The image is typical of polycrystalline NMC materials.[21] The ~10 μm particle shown consists of an aggregate of crystallites with grain size of ~1 μm. Individual crystallite grains can be seen clearly on the surface. The presence of these grains results in a rough surface with surface features in the form of pits and valleys whose depth is on the order of the same size as their crystallite size (~1 um). Figures 2b–2h shows SEM images of NMC622 particles processed with the MF method for 30 min, 1h, 2 h, 3 h, 4 h, 6 h, and 8 h, respectively. The secondary particle size had not changed after the MF process and was essentially identical to that of unprocessed NMC622. However it is apparent that the surface had been markedly smoothed compared to NMC622 as the processing time increased. The sample processed for 30 min, shown in Figure 2b, consists of a mixture of unprocessed particles and processed particles. Longer MF processing times (more than 1 h) lead to almost all the particles having
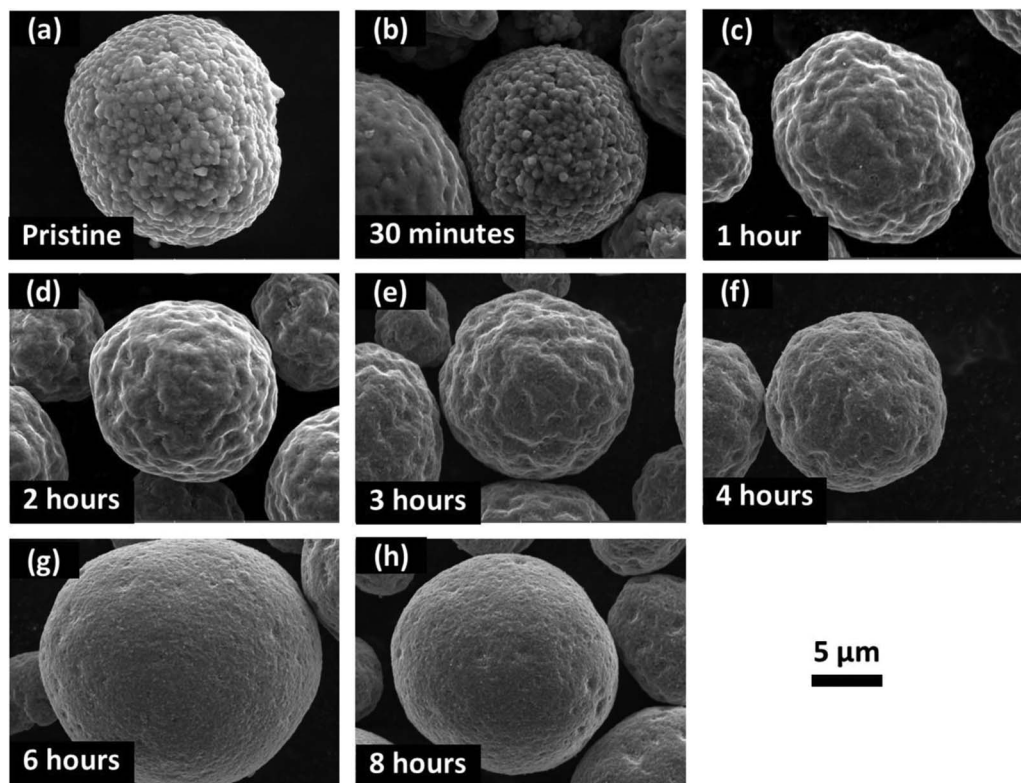

Figure 2. SEM images of (a) pristine NMC622 particles prior to mechanofusion processing and NMC622 particles processed using mechanofusion for (b) 30 min, (c) 1 h, (d) 2 h, (e) 3 h, (f) 4 h, (g) 6 h, and (h) 8 h.
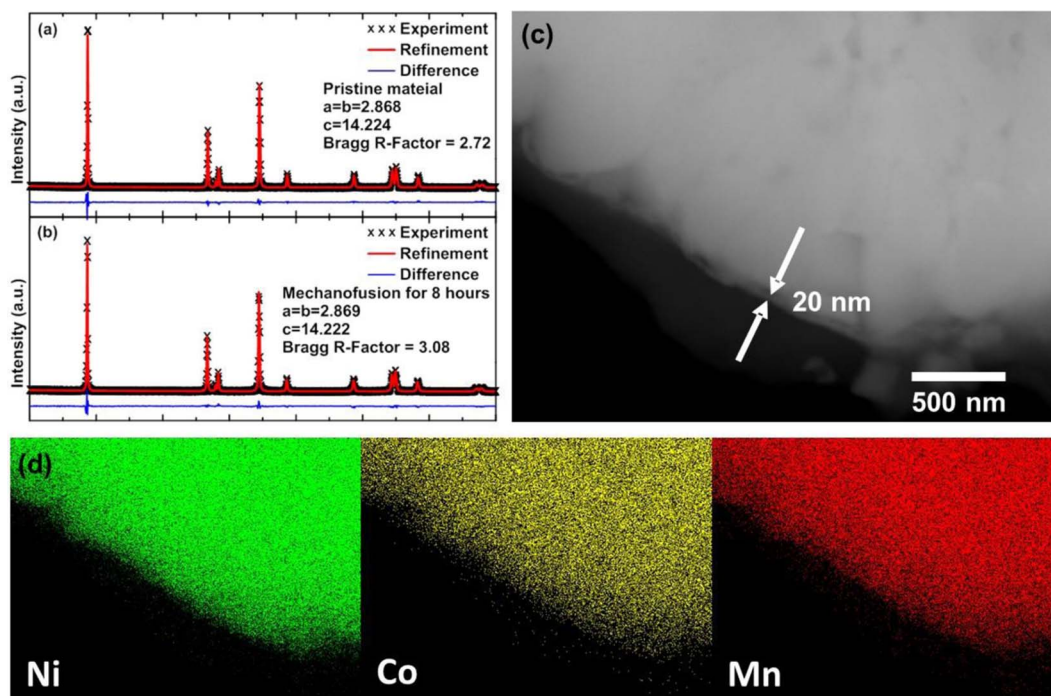
Figure 3. XRD patterns and Rietveld refinements of (a) pristine NMC622 and (b) NMC622 that has been processed using mechanofusion for 8 hours. (c) A cross-sectional SEM image and (d) EDS mapping of NMC622 after mechanofusion for 8 hours.

smoothed surfaces. The surface of the smoothed particles seems to be coated with a homogeneous and continuous coating layer, which will be discussed later. When the processing time exceeds 4 h, the original rough features of the pristine particles begins to disappear. After 8 h the particles are smooth and spherical.

Figures 3a and 3b show the XRD patterns and corresponding Rietveld refinements of pristine NMC622 and NMC622 processed using MF for 8 h. Even though the SEM images in Figure 2 show dramatic differences between the two samples, there is no observable change in the XRD patterns. Similar lattice parameters were also obtained from Rietveld refinements. This indicates that the bulk crystal structure does not change during the MF process, so that the MF process only modifies the surface of the spherical NMC622 material. Figure 3c shows an SEM image of the cross section of an NMC622 particle after 8 h of MF. A ~20 nm surface layer can be distinguished in the image. However, the thickness of this surface layer is not uniform. This is due to the rugged surface of pristine NMC622 that leads to the coating over depressions being thicker than over protuberances. Figure 3d shows the EDS map of the cross-sectional SEM image. Ni, Mn and Co are distributed homogeneously across the particle and surface coating. Considering no other surface coating additives were used during the MF process, it can be concluded that the surface coating has the same composition as the bulk material. This coating seems to have been generated by the material near the surface being smeared evenly over the particle surface by the high sheer forces during MF.

Figure 4a shows a TEM image of the edge of a particle processed using MF for 8 h. A surface coating layer is present in the TEM images, confirming the observation from SEM images. Selected area electron diffraction (SAED) was performed on a few spots randomly selected from different positions in the surface coating. All the SAED patterns are characteristic of an amorphous structure. A typical SAED pattern of the surface layer is shown in Figure 4b, where the surface coating is characterized with an amorphous halo. This supports the model that material near the particle surface is being smeared evenly over the particle surface by the high sheer forces during MF, as such a process would significantly disrupt the cathode crystal structure. To summarize, MF processing of polycrystalline NMC622 results in the smoothing of the particles and a generation of a thin

amorphous surface coating with the same metals composition as the bulk.

Figure 5a shows the voltage curves of pristine NMC622 and NMC622 MF processed for different times. All the materials have a similar first charge capacity. However, voltage hysteresis increases as the processing time increases, possibly due to a reduction in surface area and the amorphization of the surface layer.[22] The MF process also results in a slightly reduced reversible capacity, presumably due to the increased polarization and the consumption of active material form the amorphous surface layer. Figure 5b shows the cycling performance of these materials. Coin cells were cycled between 3.0 V and 4.4 V. A current rate of C/20 was used for the first cycle, for the rest cycles, cells were cycled at a C/2 rate with a 5 hour hold at the top of charge. All MF-processed materials have better capacity retention than pristine NMC622. This is ascribed to its reduced surface area, resulting in reduced parasitic reactions between cathode particles with electrolyte.[20] It is also possible that the amorphous surface coating layer partially suppresses the reaction between active material and electrolyte, leading to better cyclability.[23] As the MF time increases, only slight differences in cycling performance result, suggesting that
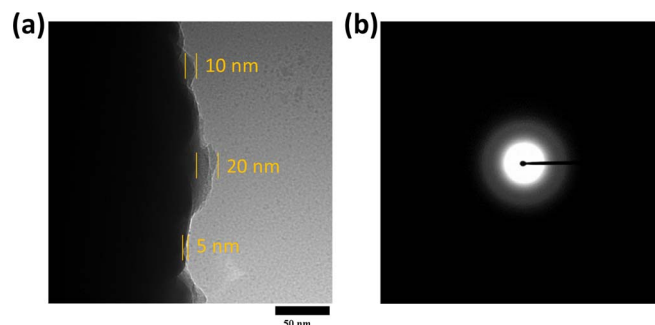

Figure 4. (a) TEM image of the edge of an NMC622 particle processed using mechanofusion for 8 hours. (b) SAED pattern of the surface coating observed in TEM.
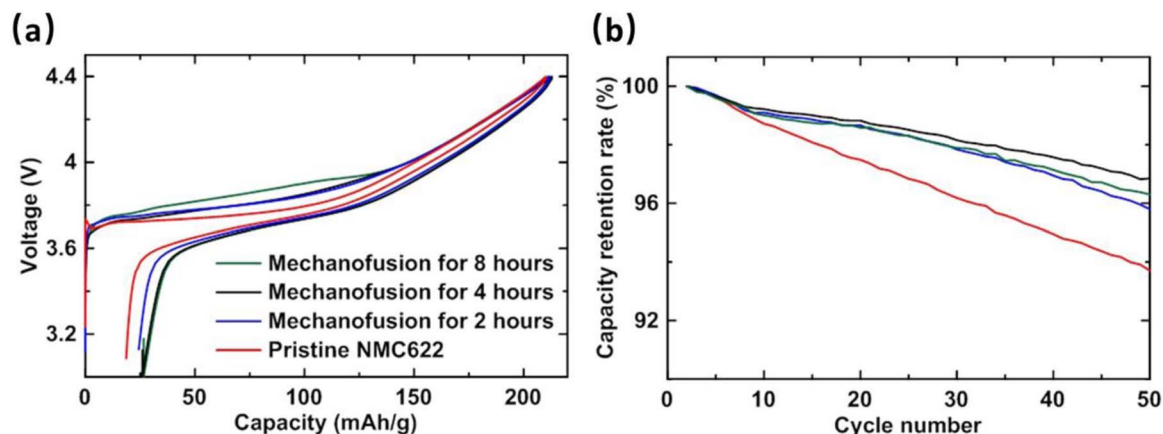
Figure 5. (a) First cycle voltage curve and (b) cycling performance of NMC622 processed using mechanofusion for different times.

only a thin coating and short processing time is needed to achieve the cycling improvement effect. Greater MF processing time results in greater cell polarization and little gain in capacity retention, if any. It should be noted that half-coin cells that employ lithium metal as counter/reference electrode have extra excess lithium and electrolyte, therefore the result obtained might not be the same as in the case of a full cell.[24] More experiments studying the compatibility of smooth cathode particles with electrolyte and negative electrode are needed for a practical evaluation.

Conclusions

A mechanofusion method was used for the first time to process cathode materials without any additives. Polycrystalline NMC622 cathode particles became smoother and more rounded after the mechanofusion process and were found to be covered with a thin amorphous layer that had the same metals composition as the bulk particle. Mechanofusion processed cathode particles had significantly improved cycling performance compared to the pristine particles, however with some increase in impedance and slightly less capacity. We believe that cathode surface reduction by mechanofusion processing represents an important method to improving cathode materials performance.

Acknowledgments

ORCID

M. N. Obrovac https://orcid.org/0000-0001-5509-3185

References

1. B. Dunn, H. Kamath, and J.-M. Tarascon, *Science*, **334**, 928 (2011).
2. R. Van Noorden, *Nature*, **507**, 26 (2014).
3. B. Xu, D. Qian, Z. Wang, and Y. S. Meng, *Mater. Sci. Eng. R Reports*, **73**, 51 (2012).
4. Z. Chen, Y. Qin, K. Amine, and Y. K. Sun, *J. Mater. Chem.*, **20**, 7606 (2010).
5. J. Vetter, P. Novák, M. R. Wagner, C. Veit, K. C. Möller, J. O. Besenhard, M. Winter, M. Wohlfahrt-Mehrens, C. Vogler, and A. Hammouche, *J. Power Sources*, **147**, 269 (2005).
6. S. Tan, Y. J. Ji, Z. R. Zhang, and Y. Yang, *ChemPhysChem*, **15**, 1956 (2014).
7. Y. K. Sun, S. T. Myung, M. H. Kim, J. Prakash, and K. Amine, *J. Am. Chem. Soc.*, **127**, 13411 (2005).
8. A. M. Wise, C. Ban, J. N. Weker, S. Misra, A. S. Cavanagh, Z. Wu, Z. Li, M. S. Whittingham, K. Xu, S. M. George, and M. F. Toney, *Chem. Mater.*, **27**, 6146 (2015).
9. L. Li, Z. Chen, Q. Zhang, M. Xu, X. Zhou, H. Zhu, and K. Zhang, *J. Mater. Chem. A*, **3**, 894 (2015).
10. B. Xiao, B. Wang, J. Liu, K. Kaliyappan, Q. Sun, Y. Liu, G. Dadheech, M. P. Balogh, L. Yang, T.-K. Sham, R. Li, M. Cai, and X. Sun, *Nano Energy*, **34**, 120 (2017).
11. S. F. Lux, T. Placke, C. Engelhardt, S. Nowak, P. Bieker, K.-E. Wirth, P. Passerini, M. Winter, and H.-W. Meyer, *J. Electrochem. Soc.*, **159**, A1849 (2012).
12. R. Pfeffer, R. N. Dave, D. Wei, and M. Ramlakhan, *Powder Technol.*, **117**, 40 (2001).
13. M. Naito, T. Hotta, and T. Fukui, *Key Eng. Mater.*, **253**, 275 (2009).
14. C. S. Chou, C. H. Tsou, and C. I. Wang, *Adv. Powder Technol.*, **19**, 383 (2008).
15. W. Chen, R. N. Dave, R. Pfeffer, and O. Walton, *Powder Technol.*, **146**, 121 (2004).
16. L. Zheng, T. D. Hatchard, and M. N. Obrovac, *MRS Commun.*, **9**, 245 (2019).
17. I. Belharouak, Y. K. Sun, J. Liu, and K. Amine, *J. Power Sources*, **123**, 247 (2003).
18. K. M. Shaju, G. V. S. Rao, and B. V. R. Chowdari, *J. Electrochem. Soc.*, **48**, 145 (2002).
19. N. Yabuuchi, Y. Koyama, N. Nakayama, and T. Ohzuku, *J. Electrochem. Soc.*, **152**, A1434 (2005).
20. T. Marks, S. Trussler, A. J. Smith, D. Xiong, and J. R. Dahn, *J. Electrochem. Soc.*, **158**, A51 (2011).
21. Y. Liu, W. Yao, C. Lei, Q. Zhang, S. Zhong, and Z. Yan, *J. Electrochem. Soc.*, **166**, A1300 (2019).
22. Z. Wang, C. Wu, L. Liu, F. Wu, L. Chen, and X. Huang, *J. Electrochem. Soc.*, **149**, A466 (2002).
23. R. S. Arumugam, Lin Ma, J. Li, X. Xia, J. M. Paulsen, and J. R. Dahn, *J. Electrochem. Soc.*, **163**, A2531 (2016).
24. E. Bjorklund, D. Brandell, M. Hahlin, K. Edstrom, and R. Younesi, *J. Electrochem. Soc.*, **164**, A3054 (2017).